

Potential of PET-MRI for imaging of non-oncologic musculoskeletal disease

Feliks Kogan¹, Audrey P. Fan¹, Garry E. Gold^{1,2,3}

¹Department of Radiology, ²Department of Bioengineering, ³Department of Orthopaedic Surgery, Stanford University, Stanford, California, USA

Correspondence to: Feliks Kogan, PhD. Department of Radiology, Stanford University, 1201 Welch Rd Stanford, CA 94305, USA.

Email: fkogan@stanford.edu.

Abstract: Early detection of musculoskeletal disease leads to improved therapies and patient outcomes, and would benefit greatly from imaging at the cellular and molecular level. As it becomes clear that assessment of multiple tissues and functional processes are often necessary to study the complex pathogenesis of musculoskeletal disorders, the role of multi-modality molecular imaging becomes increasingly important. New positron emission tomography-magnetic resonance imaging (PET-MRI) systems offer to combine high-resolution MRI with simultaneous molecular information from PET to study the multifaceted processes involved in numerous musculoskeletal disorders. In this article, we aim to outline the potential clinical utility of hybrid PET-MRI to these non-oncologic musculoskeletal diseases. We summarize current applications of PET molecular imaging in osteoarthritis (OA), rheumatoid arthritis (RA), metabolic bone diseases and neuropathic peripheral pain. Advanced MRI approaches that reveal biochemical and functional information offer complementary assessment in soft tissues. Additionally, we discuss technical considerations for hybrid PET-MR imaging including MR attenuation correction, workflow, radiation dose, and quantification.

Keywords: Positron emission tomography-magnetic resonance imaging (PET-MRI); musculoskeletal imaging; nuclear medicine; arthritis; osteoporosis

Submitted Nov 01, 2016. Accepted for publication Dec 12, 2016.

doi: 10.21037/qims.2016.12.16

View this article at: <http://dx.doi.org/10.21037/qims.2016.12.16>

Introduction

Imaging of the musculoskeletal system has benefited greatly from new technologies to image morphology and function in many tissues (1,2). This has included significant advancements in radiographic, computed tomography (CT), magnetic resonance (MRI), ultrasound, and positron emission tomography (PET) imaging methods. However, assessment of multiple tissues and functional processes are often necessary to study the complex processes in many musculoskeletal diseases, such that any one modality may not be optimal for diagnosis. To combine the strengths and overcome the limitations of various imaging modalities, hybrid imaging systems have been developed and introduced into clinical medicine. The most prominent of these are PET-CT scanners, which utilize high-resolution

CT to better localize molecular information from PET imaging (3,4). More recently, hybrid PET-MRI systems have been introduced which may be an appropriate alternative to study many musculoskeletal disorders (5,6). In addition to a lack of ionizing radiation, MRI offers superior soft tissue contrast to CT, such as in cartilage and muscle. MRI can also provide additional information regarding tissue biochemistry, diffusion, and perfusion. For these reasons, MRI is the preferred imaging modality over standalone CT for many musculoskeletal disorders.

Emerging PET-MRI systems offer an exciting new modality to simultaneously acquire numerous functional information as well as high-resolution morphology to study the complex pathogenesis in musculoskeletal disorders. In this review, we summarize PET imaging of molecular processes in non-oncologic musculoskeletal diseases and

outline the potential of hybrid PET-MR imaging for these applications. A background to PET-MRI systems and technical considerations is included.

Why PET-MRI?

New PET-MRI systems promise to combine high-resolution morphologic MR imaging with simultaneous functional information from PET to study the complex processes involved in numerous musculoskeletal disorders. PET has incomparable abilities to provide quantitative information about the molecular and metabolic activity of tissues but needs the assistance of higher-resolution, anatomic information to localize these physiologic processes. In musculoskeletal imaging, many disorders are now being recognized as affecting the multiple tissues, and can take advantage of the unique features of hybrid PET-MRI.

Molecular imaging of early disease processes

PET is the only molecular imaging modality with high sensitivity to several processes that precede these structural and biochemical changes at the tissue level (6). The molecular imaging capabilities of PET can provide vital information about the earliest metabolic changes in musculoskeletal disorders. This information is highly complementary to qualitative and quantitative information from established MRI metrics of tissue health.

Several commercially available PET tracers have already been applied to study musculoskeletal disease. The two most widely applied radiotracers for musculoskeletal imaging are ^{18}F -fluorodeoxyglucose (^{18}F -FDG) and ^{18}F -sodium fluoride (^{18}F -NaF). ^{18}F -FDG PET is a widely used marker for glucose metabolism and is sensitive to areas of acute phase cellular response (neutrophils or PMNs) such as inflammation and infection (7). ^{18}F -NaF is a long recognized bone-seeking agent that is able to probe bony remodeling (8-10).

^{18}F -FDG

^{18}F -FDG, an analog of glucose, is the most widely used PET radiotracer in clinical practice (11,12). FDG is taken up by cells through glucose transporters and then phosphorylated by hexokinase under kinetics similar to those of glucose. However, the chemistry of the FDG prevents the metabolism or catabolism of the phosphorylated FDG, effectively trapping the molecule in the cell. This results

in a buildup of ^{18}F -FDG in highly metabolic tissues that consume more glucose in order to sustain their metabolic activity. Because many tumors are hyperglycemic, FDG PET is extensively used in oncologic imaging for tumor staging and grading of several cancers. Additionally, the increased glucose utilization by activated inflammatory cells makes ^{18}F -FDG PET a useful tool to identify musculoskeletal inflammation and infection (13). ^{18}F -FDG also has some limitations. High glucose metabolism and consequent high ^{18}F -FDG uptake are not unique phenomena. As such, differentiation of the source of high glucose metabolism, e.g., between inflammation and bone remodeling, may be difficult and results in false-positive results (14).

^{18}F -NaF

^{18}F -NaF was first recognized as a bone-seeking agent in 1962 (8) and has been approved for PET imaging by the Food and Drug Administration (FDA) since 1972. The mechanism of skeletal uptake of ^{18}F -NaF is based on ion exchange (15). Bone tissue is continuously renewing itself through remodeling at the bone surface. ^{18}F ions exchange with hydroxyl ions (-OH) on the surface of the hydroxyapatite to form fluoroapatite (16). This exchange occurs at a rapid rate; however, the actual incorporation of ^{18}F ions into the crystalline matrix of bone may take days or weeks. Uptake of ^{18}F -NaF is a function of osseous blood flow and bone remodeling. ^{18}F -NaF uptake on PET images are interpreted as processes that increase exposure of the surface of bone and provide a higher availability of binding sites, such as osteolytic and osteoblastic processes (17).

High resolution and functional imaging of soft tissue

MRI is able to provide multiple different structural and functional contrasts in soft tissue that are unavailable with any other imaging modality. In the clinical setting, MRI is the primary imaging system used to diagnose injuries in soft tissues such as intervertebral disc injuries; tears in the menisci, ligaments and tendons; as well as occult bone injuries. Additionally, MRI is also widely used to study pathogenesis of many musculoskeletal disorders using advanced MRI techniques that provide unique functional information (18,19). T2 and T1rho relaxometry as well as magnetization transfer techniques provide information about cartilage biochemistry and have been shown to have significant prognostic value (20,21). Further, arterial spin

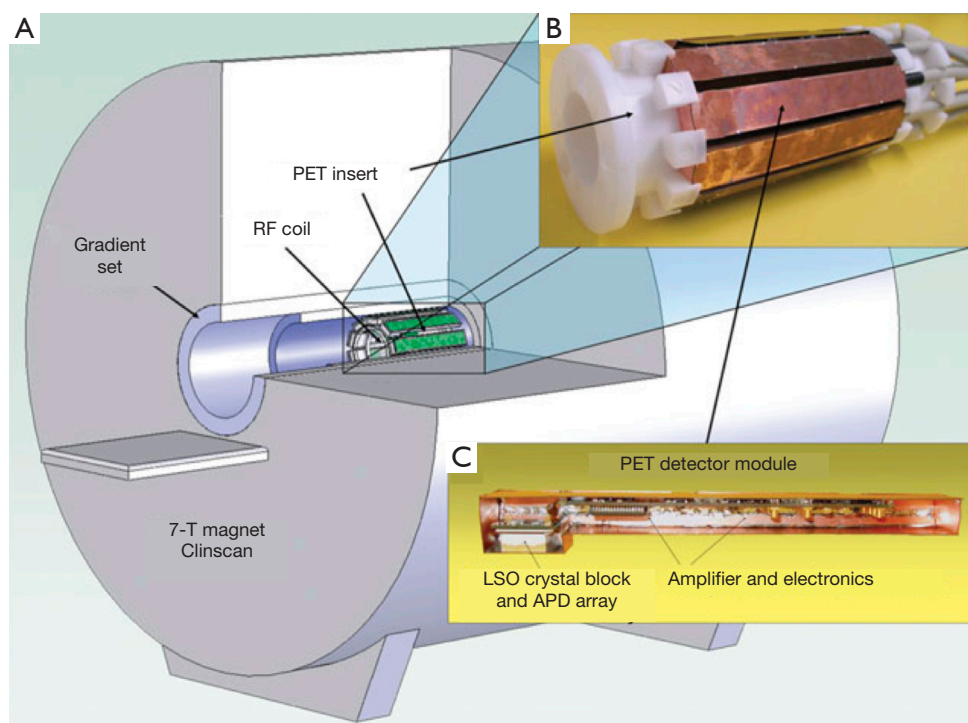


Figure 1 Schematic of integrated PET-MRI systems. (A) Concept for integration of PET and MRI: PET insert placed inside the MRI scanner, matching the centers of both fields of view. This is made possible by an (B) MRI-compatible PET insert based on APD detectors which can be positioned inside the magnet. Each (C) detector module consists of a scintillator block, APD array and preamplifier surrounded by MRI-compatible copper shielding. This model has been expanded using silicon photomultipliers (SiPMs) into 3T whole-body systems which are now commercially available from several vendors. Reprinted by permission from Macmillan Publishers Ltd: Nature Medicine (5) 2008. PET, positron emission tomography; MRI, magnetic resonance; APD, avalanche photodiode.

labeling (ASL) (22) and chemical exchange saturation transfer (CEST) (23,24) techniques are able to assess muscle perfusion and energetics, respectively. Although MRI is not typically associated with bone imaging, tissue diffusion (25) and ultra-short echo time (uTE) (26,27) methods are able to provide important information about bone strength and fracture risk. These methods as well as many other MRI applications in musculoskeletal imaging are discussed in numerous review papers on the topic (28-30). Because MRI can offer novel functional contrasts, its combination with PET offers powerful observations of distinct physiological processes occurring in bone and cartilage at the same time.

Radiation dose reduction

PET-MRI offers reduced radiation dose compared to PET-CT. Minimizing radiation exposure to patients is critical to widespread application of nuclear medicine techniques

to musculoskeletal imaging. As MRI does not produce any ionizing radiation, replacing CT with MRI can reduce the radiation dose to patients undergoing hybrid PET imaging by up to 80% (31). Further, MRI protocols (20–60 minutes) are often longer than the data collection time in one patient bed position in clinical PET-CT (3–5 minutes). As current PET-MR hybrid systems allow all of the MR scan time to be used to collect PET data, the injected dose of radiotracer can be significantly reduced. The ability to minimize radiation dose is vital for imaging of pediatric patients as well as in reproducibility and longitudinal studies.

PET-MRI systems and technical considerations

Recent advancements have overcome many technical challenges, including interference between imaging modalities, to make integrated PET-MR systems possible (Figure 1) (32,33). The main challenges revolve around

space constraints when merging the hardware into a single device, and that photomultiplier tubes (PMTs) used in conventional PET detectors do not operate properly in the presence of a magnetic field. The first attempts to solve this problem used a technically relatively simple approach to place the MRI and shielded PET components in line with a similar configuration to PET-CT (34). Unfortunately, this solution results in long scan times, as it does not allow for simultaneous acquisitions. While this may be a viable solution for small-animal imaging, a system capable of performing simultaneous PET and MRI acquisitions is optimal. Fortunately, the emergence of robust MRI-compatible solid state photodetectors such as avalanche photodiodes (APDs) (35) and more recently silicon photomultipliers (SiPMs) (36) has made truly simultaneous PET-MRI possible. These detectors are essentially insensitive to large magnetic fields, which has allowed for the integrated PET-MRI systems. Further, these devices have other desirable resolution properties compared with PMTs, which has allowed these integrated PET-MRI systems to feature the most advanced PET acquisitions.

In addition to the integration of hardware components, there are also several technical considerations for simultaneous PET-MRI imaging that need to be addressed. The most pressing of these is how to account for attenuation of PET photons using MR images, and is discussed below.

PET attenuation correction (AC)

Besides the complexity to integrate hardware for multiple imaging modalities, PET-MRI faces challenges with AC compared to PET-CT. In order to obtain accurate PET uptake quantification, emission data recorded during a PET scan must be corrected for tissue and hardware attenuation. This is performed during reconstruction using an attenuation map (μ -map). Because the mechanism for image formation in CT is similar to that of PET, high-resolution CT images in a PET-CT can be easily transformed to linear attenuation maps.

However, as MR images are based on proton density, MR-based correction of PET photon attenuation (MRAC) is less established. This is an active area of study and several methods have been developed for AC based on MR acquired information (37,38). Most commercial systems use a segmentation approach to account for PET attenuation from fat and water tissue using Dixon fat-water separated images and known AC coefficients. However, this

segmentation approach does not account for attenuation due to bone. Cortical bone, which is an important area of study in musculoskeletal disease, has higher attenuation of PET photons than soft tissue, but it is difficult to account for on MRAC due to its lack of signal on conventional MR images. Methods utilizing fast MRI acquisition techniques such as uTE and zero echo time (zTE) have been proposed to characterize and correct for cortical bone attenuation.

AC for MRI radiofrequency (RF) coils is another challenge in simultaneous PET-MR imaging systems (39,40). AC of these hardware components is required as their presence leads to considerable attenuation of the PET signal (37). Rigid and stationary MR hardware components, such as the patient table, are corrected for by integrating CT-based attenuation templates of these parts at a fixed position in the μ -map used for AC in PET image reconstruction (38). However, flexible RF coils, which are popular for PET-MR imaging due to their reduced attenuation of PET photons, are currently disregarded in MRAC since their position and individual geometry are unknown in patient scans. Investigations are ongoing to account for the presence of these coils on MRAC maps.

Workflow considerations for PET-MRI

An important first consideration in PET-MRI workflow is the time of tracer injection and subsequent time of imaging. Fluorine-18 (^{18}F) labeled radiotracers such as ^{18}F -FDG and ^{18}F -NaF have advantageous tracer kinetics, which have aided in its widespread application. Fluorine-18 has a favorable half-life of approximately 110 minutes, which does not require an on-site cyclotron (it can be manufactured commercially and shipped to imaging centers) but is short enough to minimize the effective radiation dose to the subject. ^{18}F -FDG PET is typically imaged 60–75 minutes after tracer injection (41). On the other hand, several unique characteristics of ^{18}F -NaF make it a desirable radiotracer for imaging of bone. ^{18}F -NaF has minimal binding to serum proteins, which allows a rapid single-pass extraction and fast clearance from the soft tissues. This high bone uptake and faster soft-tissue clearance lead to a higher quality of images with high bone-to-background ratio and allow for shorter imaging times. ^{18}F -NaF PET imaging can be performed less than 1 hour after injection (15).

The total PET-MRI scan time is often limited by MRI acquisition times and will depend on which areas need to be imaged. Whole-body protocols, e.g., to study musculoskeletal pain, have been proposed that acquire 5–6 “bed” positions, each 3–5 minutes that include a combination of anatomical

and functional MRI scans (42,43). Designated protocols where the anatomy of interest is contained in one PET bed, e.g., for the knee, permit longer MRI protocols and the duration of scan time to be used to acquire PET data. This allows for higher SNR PET images as well as a reduction in radiotracer dose as discussed before. All PET-MRI bed positions that are scanned need an accompanying scan for MR-based attenuation correction, and different correction techniques may be applied to different parts of the body.

Quantification and interpretation of PET signal

PET imaging offers high sensitivity to molecular contrasts, which can greatly benefit musculoskeletal imaging. However, proper interpretation of PET signal requires an understanding of the tracer uptake mechanisms. The most common way to quantify PET tracer accumulation is by standardized uptake values (SUV), the tissue activity concentration normalized by the fraction of the injected dose/unit weight. SUV provides a semi-quantitative measure of PET radiotracer uptake. While this method has been shown to be reproducible and reliable, it can be affected by several biologic and physical factors (44,45). Caution should be taken when comparing SUV between different patient cohorts or in longitudinal evaluation of musculoskeletal disease.

Kinetic modeling

A more quantitative approach to PET image analysis is available by imaging during the tracer administration and reconstructing dynamic frames of the PET acquisition. Through pharmacokinetic modeling, the dynamic PET scans can then be used to quantify rate parameters that describe the movement of tracer between blood, extracellular and intracellular compartments. These rate constants can provide more quantitative measures of tissue uptake as well as additional information about underlying processes (blood flow versus bone mineralization) that drive tracer uptake. The tracer rate constants are quantitative and can be compared between patient populations. The use of kinetic modeling for ^{18}F -FDG and ^{18}F -NaF in musculoskeletal systems has been previously reviewed in several publications (46-48).

The PET-MRI system may better enable kinetic modeling through more accurate quantification of the arterial input function (AIF), e.g., the amount of tracer input in arterial blood. Although some studies have derived

input functions from large regions of interest such as the aorta, more targeted vessels are arguably more accurate (e.g., the popliteal artery for the knee). These vessels may also be the only ones in the field of view for some PET-MRI applications. While AIF curves from dynamic PET images alone may suffer from partial volume problems, more accurate quantification is available if the vessel volume is known (e.g., from high-resolution MRI angiograms) (49). Estimation of an accurate AIF is necessary for quantification of rate parameters.

Applications

While hybrid PET-MRI musculoskeletal imaging is in its nascent stages, there are many applications that could benefit from this multimodal approach. The following review was compiled to present a broad overview of novel clinical and basic science applications of MRI and PET to several, widely prevalent musculoskeletal disorders. A high-level PubMed search was used to determine both widely applied techniques as well as novel emerging methods and applications. Any early applications of hybrid PET-MRI musculoskeletal imaging were included. As hybrid PET-MRI is a new and emerging field, we focused on the potential applications of this multimodal approach without any biases to specific methods or tracers.

Osteoarthritis (OA)

OA is a chronic degenerative disease affecting all tissues in the joint. OA remains a leading cause of disability, affecting more than half the population over the age of 65. Despite its prevalence, pathogenesis in OA is still poorly understood. There is great need for imaging biomarkers of early changes in OA in order to better understand the disease process as well as to develop new therapies (50,51).

MRI has long been utilized to non-invasively study and understand many of the complex disease processes involved in OA (52). MRI provides excellent high-resolution morphologic information of joint tissue. This, along with its ability to produce multiple different contrasts, has made MRI an invaluable tool to study tissue changes associated with OA. Various endogenous contrast methods can be used to assess soft tissue health (e.g., cartilage morphology, menisci and major ligaments, and joint effusion) and even changes in bone [e.g., subchondral bone marrow lesions (BMLs) and cysts, osteophytes, and bone attrition]. Further, delayed-contrast enhanced MR imaging (DCE-MRI) can

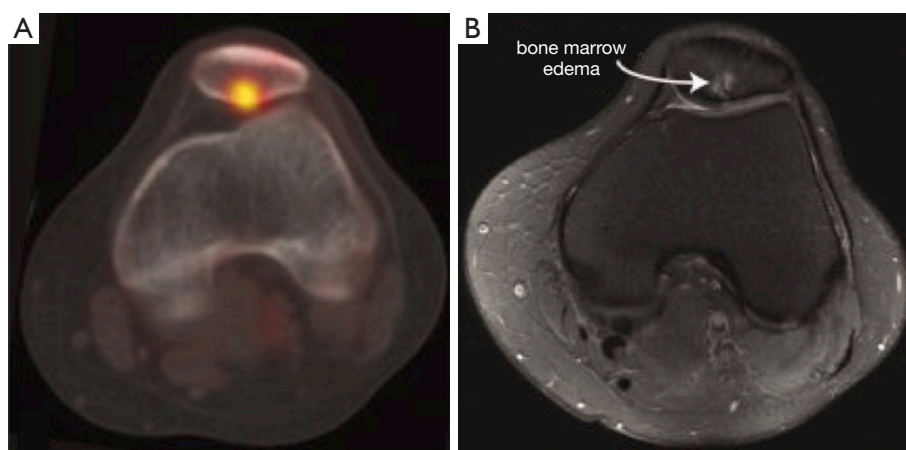


Figure 2 Concordance between bone abnormalities on MRI and increased ^{18}F -NaF uptake on PET. (A) Fused ^{18}F -NaF PET/CT and (B) MRI image of the patellofemoral joint a subject with patellofemoral pain. Bone marrow edema identified on MRI in the apex of the patella corresponded to increased ^{18}F -NaF PET uptake. Simultaneous PET/MRI systems present an opportunity to study the role metabolic activity in structural MRI findings widely used to assess OA progression. From reference (69), with permission. ^{18}F -NaF, ^{18}F -sodium fluoride; PET, positron emission tomography; CT, computed tomography; MRI, magnetic resonance; OA, osteoarthritis.

be used to assess synovitis (53). Semi-quantitative scoring systems that characterize OA pathological features based on MRI have been shown to predict OA disease progression (54,55).

However, structural degenerative changes observed on MRI are likely at a late stage in the disease process when tissue loss has already occurred and treatments are unlikely to be effective. Anatomical MRI contrasts are unable to assess the underlying mechanisms that trigger the disease. As an alternative, advanced quantitative MRI techniques, such as T_2 (56,57) or $T_{1\rho}$ (58,59) relaxation times, delayed gadolinium-enhanced MRI of cartilage (dGEMRIC) (60,61), and CEST of glycosaminoglycans (gagCEST) (62,63) can provide biochemical tissue information about collagen matrix organization, glycosaminoglycan (GAG) content, and hydration. The application of these techniques has largely been limited to articular cartilage. However, bone is difficult to study with MRI due to the extremely short lifetimes (T_2) of the protons (tightly bound water and collagen), which makes it ordinarily invisible in MR images. While bone structure can be inferred from the signal of the surrounding soft tissues, its lack of signal makes functional imaging of bone structures infeasible with MRI.

^{18}F -NaF PET can assess the metabolic activity of subchondral bone remodeling. Increased bone remodeling has been implicated as a mechanism of OA progression that leads to changes in bone as well as in adjacent

cartilage (64,65). This makes ^{18}F -NaF an intriguing marker to study the role of subchondral bone changes in OA pathogenesis. High ^{18}F -NaF uptake has often been observed in degenerative and arthritic knees during evaluation of osseous metastatic disease. ^{18}F -NaF PET may also be useful in the detection of bone remodeling in early stage OA of the temporomandibular and hip joints (17,66). SUV_{max} was significantly higher in hip joints with an abnormal finding in bone on MRI (67). Additionally, ^{18}F -NaF has been used as a marker of pain. Increasing severity of hip pain was shown to correlate with increasing SUV_{max} (67). Furthermore, subjects with patellofemoral pain exhibited elevated bone metabolic activity at the patellofemoral joint (68). Bone abnormalities (edema, cysts, etc.) on MRI tended to coincide with regions of increased tracer uptake on the ^{18}F -NaF PET scans (Figure 2) (69). However, increased bone activity on ^{18}F -NaF PET did not always correspond to structural damage in the bone or cartilage as seen on MRI, suggesting that ^{18}F -NaF imaging provides distinct information in patellofemoral pain patients (69).

^{18}F -FDG offers a different metabolic contrast to study the role of inflammation in OA disease progression. Synovitis, inflammation of the synovial membrane, is increasingly recognized as an important feature of the pathophysiology of OA (70,71). Previous studies using FDG-PET evaluated patients with clinically diagnosed shoulder and knee OA (72,73). A diffuse increase in FDG

uptake was observed in patients compared to healthy volunteers, which the authors interpreted as the presence of synovitis. BMLs also play a role in the progression of OA and are usually identified on MRI. While the etiology of BMLs is likely multifactorial, they are thought to have an inflammatory component (74). FDG-PET may offer a marker to study the inflammatory mechanisms that underlie these lesions.

Hybrid PET-MRI systems allow for comprehensive imaging of the whole joint, including soft tissues and bone, which is necessary to study complex disease processes in OA. PET imaging with ^{18}F -fluoride and ^{18}F -FDG offers metabolic information regarding bone remodeling and inflammatory processes. This information can be used in combination with biochemical and structural information from soft tissues on MRI to assess spatial relationships between tissues during OA disease pathogenesis. Initial experiences with hybrid PET/MR systems have shown that metabolic activity varies between different types of subchondral bone pathology identified on MRI. This can enhance our understanding of semi-quantitative MRI scoring systems, which are widely used. Furthermore, ^{18}F -fluoride may identify abnormalities in subchondral bone metabolic activity before structural changes are seen on MRI (75,76).

Rheumatoid arthritis (RA)

RA is a systemic inflammatory autoimmune disorder, which affects both large and small joints. Although heterogeneous, RA is primarily characterized by symmetric, erosive synovitis, which leads to the destruction of cartilage and, eventually, underlying bone. In comparison with OA, RA typically progresses more rapidly. Radiographs have long been used for diagnosis of RA but rely on detection of late stage disease processes such as bone erosions or joint space narrowing. Optimal patient outcomes depend on aggressive treatment with anti-inflammatory drugs early in the disease process. Thus, novel methods to image RA have revolved around early-detection methods and monitoring of treatment response.

As inflammation is a key component to RA pathogenesis, FDG-PET is a logical molecular imaging marker to study the disease (77). In fact, FDG has been applied to studying RA in all segments of the disease cycle. Strong correlations have been cited between PET observations (e.g., number of PET positive joints and cumulative SUV) and underlying disease activity (*Figure 3A,B*) (78). Further, it has been

shown that early changes in regional FDG uptake in RA patients undergoing anti-TNF- α (infliximab) treatment were related to global disease activity in later clinical assessment. Animal models of RA have also been used to show that areas of increased FDG uptake correlated with future bone destruction and pannus formation seen on histology (80). While these preliminary studies suggest that FDG is highly predictive of early disease activity, larger studies are needed to confirm that these findings predict clinical outcomes.

One limitation with FDG PET is that the tracer detects glucose metabolism but may not be specific to inflammation. Alternatively, other PET radiotracers can track different processes such as cellular proliferation (i.e., by ^{11}C -Choline). Previous work has evaluated PET scans with ^{11}C -Choline and FDG in relation to synovial volume to characterize RA changes (81). A direct marker of inflammation, such as ^{11}C -(R)-PK11195 that tags macrophages in the inflammatory pathway, may offer more specific molecular targets to study RA (82,83).

MRI has similarly been developed for early detection of RA and to assess disease severity. Unlike PET, MRI provides high-resolution anatomical images to assess structural changes (e.g., peri-articular erosions, BMLs and synovial thickening) for diagnosis and staging of RA disease (*Figure 3C,D*) (79). Contrast enhancement following injection of gadolinium can further differentiate active inflammation from synovitis. Compared with radiographs, MRI offers tomographic information of various contrast methods to provide better visualization and differentiation of soft tissue. Further, MRI's advanced capabilities for early identification of bone erosions are important considerations for choice of treatment (84). For patients undergoing treatment, scoring systems that evaluate the features of RA from MRI show great potential for monitoring response to therapy (85). Lastly, new MRI methods, such as measurement of apparent diffusion coefficient (ADC) and pharmacokinetic modeling of Gadolinium enhancement and washout, offer quantitative metrics to more precisely study RA pathogenesis (86).

Hybrid PET imaging offers the potential to enhance the utility of nuclear medicine techniques to study RA. Studies with PET/CT have shown the importance of FDG uptake in differentiating enteropathies from synovitis in RA conditions (82). The use of FDG reveals clinical inflammation in a majority of RA-affected joints and with greater FDG uptake than comparable OA regions (87). Hybrid PET-MRI systems additionally offer high-resolution

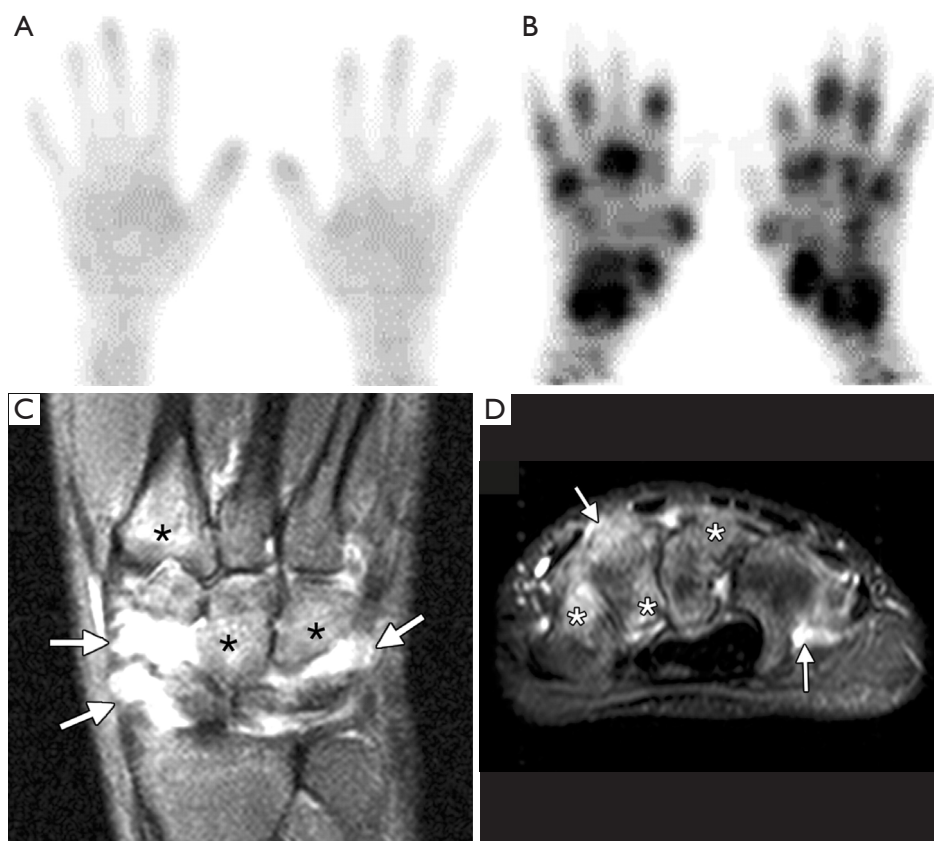


Figure 3 PET and MRI imaging of rheumatoid arthritis in the hand. (A,B) 3D projection image of ^{18}F -FDG uptake in a (A) healthy subject and (B) a subject with rheumatoid arthritis of the hand and wrist (78) [This research was originally published in *JNM*. Beckers C, Ribbens C, André B, Marcelis S, Kaye O, Mathy L, Kaiser MJ, Hustinx R, Foidart J, Malaise MG. Assessment of disease activity in rheumatoid arthritis with $(^{18}\text{F})\text{F}$ -FDG PET. *J Nucl Med* 2004;45:956-64. © by the Society of Nuclear Medicine and Molecular Imaging, Inc.]. ^{18}F -FDG PET can assess the metabolic activity of synovitis and has been correlated with underlying disease activity. (C,D) MRI. (C) Coronal STIR and (D) axial fat-suppressed T2-weighted images of a subject with early rheumatoid arthritis of the wrist and normal radiographic findings. Synovitis can be observed as high signal intensity (arrows) as can bone marrow edema (asterisks) [Narváez JA, Narváez J, De Lama E, De Albert M. MR imaging of early rheumatoid arthritis. *Radiographics* 2010;30:143-63. (79) with permission]. MRI provides high-resolution anatomical images to assess structural changes for diagnosis and staging of RA disease. Hybrid PET-MRI systems offer to combine high-resolution morphologic images with early molecular markers to enhance the study of RA. ^{18}F -FDG, ^{18}F -fluorodeoxyglucose; PET, positron emission tomography; MRI, magnetic resonance; RA, rheumatoid arthritis.

morphologic images and multiple contrasts in soft tissue to enhance the study of RA (88). In a recent study, true hybrid PET/MRI was performed in early hand RA; FDG uptake corresponded to sites of synovitis and tenovaginitis as identified on contrast-enhanced MRI, demonstrating the feasibility of PET-MRI to image inflammation in RA (89).

Metabolic bone disorders

Metabolic bone diseases include many hereditary and

acquired conditions of diverse etiology that affect bone strength, and can lead to fragility fractures, bone deformities and serious disability if untreated. These diseases are usually caused by abnormalities of vitamins or minerals, bone mass or bone structure. The most common of these disorders include osteoporosis, osteomalacia, Paget's disease and parathyroid disorders. Clinical imaging of metabolic bone disorders aims to assess bone structure and bone mass in order to gauge fracture risk. Conventional radiographs are most commonly used to evaluate bone

structure. Bone mass is also commonly measured using digital X-ray radiogrammetry (DXR) and dual energy X-ray absorptiometry (DEXA). However, bone strength not only depends on its mass but also on trabecular bone architecture, bone quality and bone geometry. Non-invasive imaging methods that can measure these bone properties are necessary to better determine future fracture risk.

The metabolic imbalance of catabolic (removal of old or damaged bone) and anabolic (growth of new bone) processes may underlie many metabolic bone diseases. Regional assessment of bone metabolism with ^{18}F -NaF PET is thus attractive (90). Small animal studies on estrogen deficiency in mice showed a strong correlation between ^{18}F -NaF PET and histomorphometric measurements, indicating that bone microdamage was significantly increased after estrogen depletion (91). Cumulative microdamage is a key component in osteoporosis pathogenesis and ^{18}F -NaF PET may be a noninvasive means to detect bone microdamage *in vivo*. For instance, quantitative dynamic ^{18}F -NaF PET has also been used to study age-related changes in bone turnover in pre- and postmenopausal women (16,92). Bone metabolism and fluoride binding to bone mineral were both significantly reduced in osteoporosis, whereas at the same time biochemical markers of bone turnover (bone-specific alkaline phosphatase) were increased. This somewhat surprising result highlights the importance of regional measurements of bone turnover (from imaging) to improve the understanding of metabolic bone diseases.

PET imaging with ^{18}F -FDG has shown potential in differentiating traumatic fractures from pathologic fractures due to malignancies. Interestingly, several studies have shown acute osteoporotic or traumatic fractures do not show elevated uptake of ^{18}F -FDG (93,94). On the other hand, the increased glucose utilization of macrophages and other active inflammatory cells results in increased FDG uptake in fractures driven by malignant or infectious bone processes. Thus, ^{18}F -FDG could potentially be used to differentiate fracture etiology throughout the entire skeletal system.

MRI has been applied to high-resolution imaging of bone structure as well as quantitative measures of bone quality and strength (95,96). Unlike most methods that image bone structure, trabecular and cortical bone is mostly visualized with negative contrast on MRI. The trabecular network can be visualized as signal void surrounded by high-signal-intensity fatty bone marrow (30). This signal void is due to the low water content and very short T2 relaxation time of bone as well as susceptibility effects at

the bone–bone marrow interface. In addition to providing high-resolution morphological images, MR is able to characterize bone quality through measures of cortical bone water and bone marrow composition. *uTE* MRI methods use radial sampling strategies to achieve <1 ms echo times to directly image the short-T2 water content of cortical bone as a surrogate of bone porosity (97,98). *uTE* scans have been shown to correspond to measures of bone quality and strength in bone specimens (98). Further, studies have shown that pore water increases in populations with increased fracture risk, including post-menopausal women and patients undergoing dialysis (99,100).

By combining structural, functional and metabolic information, PET-MRI has the ability to improve the quantitative assessment of bone strength and fracture risk. Currently, finite element (FE) analysis models are being developed to improve accuracy of bone strength estimates (101,102). MRI-based FE models use high-resolution MRI images to acquire tissue structure along with element material definitions derived from experimental tests of mechanical properties (103,104). The FE model is then virtually compressed under various simulated loads to determine measures of strength and stiffness. Metabolic information from PET about bone remodeling has the potential to improve MRI-based FE models and better quantify bone strength.

Pain generators and peripheral nerve imaging

Pain, both acute and chronic, is the most common reason patients seek medical attention. However, diagnosis and characterization of pain is challenging. Clinical assessment of pain is usually dependent on a patient's self-analysis, which is highly subjective. Current clinical imaging of pain relies on identifying anatomic abnormalities that may be producing a patient's clinical symptoms. However, structural abnormalities are often non-specific and are often present in asymptomatic patients with a similar prevalence (105,106). There is a great need for imaging tools that can identify pain-related nociceptive activity.

Molecular imaging of abnormal biological processes associated with pain has been promising to identify pain-generating pathology. FDG PET imaging can image the increased glucose metabolism utilized by inflamed or overactive neurons as a marker of neural activity. Studies in a rat model that used unilateral injury to induce neuropathic limb pain showed increased FDG uptake in injured nerves, but no increase in FDG uptake in the contralateral limb

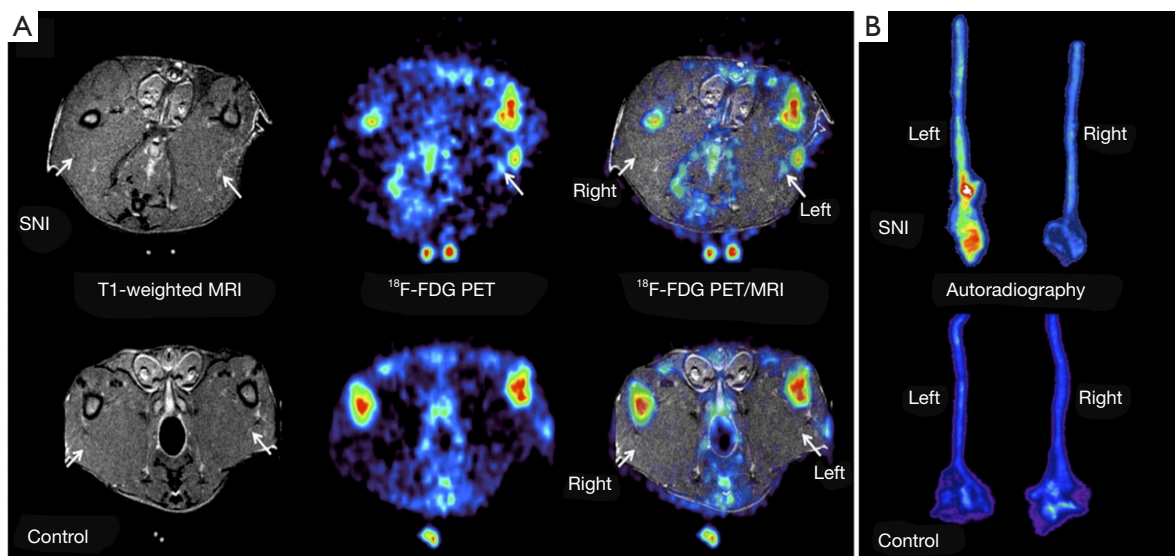


Figure 4 FDG uptake in rat model of neuropathic limb pain. (A) Representative spared-nerve injury (SNI) (top row) and control (bottom row) animals on transaxial MRI, PET, and PET/MRI with labelled sciatic nerves (arrows). Significantly increased ¹⁸F-FDG uptake is seen on the side with spared-nerve injury (left) compared with the control side (right). No significant differences between sides are observed in control animal sciatic nerves. (B) Autoradiography of sciatic nerve specimens from spared-nerve injury animals showed that normalized radiotracer uptake is higher in the injured sciatic nerve (left) than in the control sciatic nerve (right). PET/MRI offers to combine molecular information to localize neuropathic pain with MRI which is able to provide high-resolution visualization of anatomical abnormalities (107). [This research was originally published in *JNM*. Behera D, Jacobs KE, Behera S, Rosenberg J, Biswal S. (18F)-FDG PET/MRI can be used to identify injured peripheral nerves in a model of neuropathic pain. *J Nucl Med* 2011;52:1308-12. © by the Society of Nuclear Medicine and Molecular Imaging, Inc.]. MRI, magnetic resonance; PET, positron emission tomography; ¹⁸F-FDG, ¹⁸F-fluorodeoxyglucose.

or in control asymptomatic animals (*Figure 4*) (107). Additionally, in a human subject presenting with progressive difficulty walking, increased FDG uptake was observed in his lower spinal cord and sciatic nerves (108). Biopsy of the tissues confirmed the pathologic signs of neuropathy. In addition to FDG, several other molecular PET tracers are being evaluated to image pain-related nociceptive activity. These include ¹¹C-PK11195 to image activated microglia and macrophages in neuroinflammation (109), and ¹⁸F-FTC-146, a new marker of sigma 1 receptors to directly assess signaling pathways involved in pain (110).

Direct MR imaging of pain has relied on tracking of macrophages with small particles of iron oxide (SPIO). Tagged with SPIOs, macrophages have been shown to traffic to a site of nerve injury in animal models. However, these have yet to be applied in humans (111). In addition, MRI has long been used for high-resolution imaging of peripheral nerves. Clinical evaluation usually involves identification of inflammation around nerves as high signal on fat-suppressed T2-weighted images. Fat-suppressed

T1-weighted can also be used for morphology and to differentiate injured nerves from blood vessels. MRI has been used to identify entrapment neuropathies, plexus lesions and nerve compression syndromes (112,113). However, while MRI can provide high resolution imaging of peripheral nerve abnormalities, it has low specificity to identify the inciting nerve inflammation or injury.

Hybrid PET-MRI systems offer to combine the strength of each individual imaging modality and overcome the weakness of the other. PET offers molecular information to localize neuropathic pain while MRI is able to provide high-resolution to visualize anatomical abnormalities. Early experiences with hybrid PET-MR imaging in patients suffering from chronic lower extremity neuropathic pain showed FDG uptake could be localized to affected nerves and impacted clinical management of their pain (114).

Challenges and alternative imaging methods

This review has focused on the potential for hybrid PET-

MRI in non-oncologic musculoskeletal applications. Many of the challenges of simultaneous PET-MRI, including quantification, attenuation correction, and workflow considerations, are discussed in the technical considerations above. The standalone PET and MRI techniques discussed in the applications section above also have challenges, such as sensitivity to field inhomogeneities or the need for motion correction, which would feature into PET-MRI studies that utilize these methods. Additionally, there are many other imaging methods that have shown potential for solving some of the complex problems discussed above that were not discussed (2). This includes single-photon emission computed tomography (SPECT) for imaging of infection or bone turnover (115), high-resolution peripheral quantitative computed tomography (pQCT) for assessment of bone mineral density (116), as well as ultrasound (117) and optical methods (118).

Conclusions

Together, hybrid PET-MRI systems offer the potential to obtain metabolic, morphologic and functional information from all tissues to aid the study of musculoskeletal disease diagnosis and pathogenesis as well as determine targets for disease modifying therapies.

Acknowledgements

Funding: This work was supported by a National Institute of Health (NIH) (Grant R01EB002524, K24AR062068) and research support from GE Healthcare.

Footnote

Conflicts of Interest: The authors receive research support from GE Healthcare.

References

1. Gold G, Shapiro L, Hargreaves B, Bangerter N. Advances in musculoskeletal magnetic resonance imaging. *Top Magn Reson Imaging* 2010;21:335-8.
2. Wilmot A, Gieschler S, Behera D, Gade TP, Reumann MK, Biswal S, Mayer-Kuckuk P. Molecular imaging: an innovative force in musculoskeletal radiology. *AJR Am J Roentgenol* 2013;201:264-77.
3. Brady Z, Taylor ML, Haynes M, Whitaker M, Mullen A, Clews L, Partridge M, Hicks RJ, Trapp JV. The clinical application of PET/CT: a contemporary review. *Australas Phys Eng Sci Med* 2008;31:90-109.
4. Griffeth LK. Use of PET/CT scanning in cancer patients: technical and practical considerations. *Proc (Bayl Univ Med Cent)* 2005;18:321-30.
5. Judenhofer MS, Wehrl HF, Newport DF, Catana C, Siegel SB, Becker M, Thielscher A, Kneilling M, Lichy MP, Eichner M, Klingel K, Reischl G, Widmaier S, Röcken M, Nutt RE, Machulla HJ, Uludag K, Cherry SR, Claussen CD, Pichler BJ. Simultaneous PET-MRI: a new approach for functional and morphological imaging. *Nat Med* 2008;14:459-65.
6. Chaudhry AA, Gul M, Gould E, Teng M, Baker K, Matthews R. Utility of positron emission tomography-magnetic resonance imaging in musculoskeletal imaging. *World J Radiol* 2016;8:268-74.
7. Hong YH, Kong EJ. (18F)Fluoro-deoxy-D-glucose uptake of knee joints in the aspect of age-related osteoarthritis: a case-control study. *BMC Musculoskelet Disord* 2013;14:141.
8. Blau M, Nagler W, Bender MA. Fluorine-18: a new isotope for bone scanning. *J Nucl Med* 1962;3:332-4.
9. Jadvar H, Desai B, Conti PS. Sodium 18F-fluoride PET/CT of bone, joint, and other disorders. *Semin Nucl Med* 2015;45:58-65.
10. Ohnona J, Michaud L, Balogova S, Paycha F, Nataf V, Chauchat P, Talbot JN, Kerrou K. Can we achieve a radionuclide radiation dose equal to or less than that of 99mTc-hydroxymethane diphosphonate bone scintigraphy with a low-dose 18F-sodium fluoride time-of-flight PET of diagnostic quality? *Nucl Med Commun* 2013;34:417-25.
11. Etchebehere EC, Hobbs BP, Milton DR, Malawi O, Patel S, Benjamin RS, Macapinlac HA. Assessing the role of (1)(8)F-FDG PET and (1)(8)F-FDG PET/CT in the diagnosis of soft tissue musculoskeletal malignancies: a systematic review and meta-analysis. *Eur J Nucl Med Mol Imaging* 2016;43:860-70.
12. Schelbert HR, Hoh CK, Royal HD, Brown M, Dahlbom MN, Dehdashti F, Wahl RL. Procedure guideline for tumor imaging using fluorine-18-FDG. *Society of Nuclear Medicine. J Nucl Med* 1998;39:1302-5.
13. Crymes WB, 2nd, Demos H, Gordon L. Detection of musculoskeletal infection with 18F-FDG PET: review of the current literature. *J Nucl Med Technol* 2004;32:12-5.
14. Costelloe CM, Murphy WA Jr, Chasen BA. Musculoskeletal pitfalls in 18F-FDG PET/CT: pictorial review. *AJR Am J Roentgenol* 2009;193:WS1-13, Quiz S26-30.

15. Czernin J, Satyamurthy N, Schiepers C. Molecular mechanisms of bone ^{18}F -NaF deposition. *J Nucl Med* 2010;51:1826-9.
16. Schiepers C, Nuyts J, Bormans G, Dequeker J, Bouillon R, Mortelmans L, Verbruggen A, De Roo M. Fluoride kinetics of the axial skeleton measured in vivo with fluorine-18-fluoride PET. *J Nucl Med* 1997;38:1970-6.
17. Kobayashi N, Inaba Y, Tateishi U, Yukizawa Y, Ike H, Inoue T, Saito T. New application of ^{18}F -fluoride PET for the detection of bone remodeling in early-stage osteoarthritis of the hip. *Clin Nucl Med* 2013;38:e379-83.
18. Du J, Takahashi AM, Chung CB. Ultrashort TE spectroscopic imaging (UTESI): application to the imaging of short T2 relaxation tissues in the musculoskeletal system. *J Magn Reson Imaging* 2009;29:412-21.
19. Welsch GH, Mamisch TC, Hughes T, Zilkens C, Quirbach S, Scheffler K, Kraff O, Schweitzer ME, Szomolanyi P, Trattnig S. In vivo biochemical 7.0 Tesla magnetic resonance: preliminary results of dGEMRIC, zonal T2, and T2* mapping of articular cartilage. *Invest Radiol* 2008;43:619-26.
20. Staroswiecki E, Granlund KL, Alley MT, Gold G, Hargreaves BA. T2 Maps and Diffusion-Weighted Imaging of Knee Cartilage with a DESS Sequence at 3T. *Proc. Intl Soc Mag Reson Med* 2010;18:824.
21. Singh A, Haris M, Cai K, Kogan F, Hariharan H, Reddy R. High resolution T1rho mapping of in vivo human knee cartilage at 7T. *PloS one* 2014;9:e97486.
22. Englund EK, Rodgers ZB, Langham MC, Mohler ER, 3rd, Floyd TF, Wehrli FW. Measurement of skeletal muscle perfusion dynamics with pseudo-continuous arterial spin labeling (pCASL): Assessment of relative labeling efficiency at rest and during hyperemia, and comparison to pulsed arterial spin labeling (PASL). *J Magn Reson Imaging* 2016;44:929-39.
23. Kogan F, Haris M, Singh A, Cai K, Debrosse C, Nanga RP, Hariharan H, Reddy R. Method for high-resolution imaging of creatine in vivo using chemical exchange saturation transfer. *Magn Reson Med* 2014;71:164-72.
24. Kogan F, Haris M, Debrosse C, Singh A, Nanga RP, Cai K, Hariharan H, Reddy R. In vivo chemical exchange saturation transfer imaging of creatine (CrCEST) in skeletal muscle at 3T. *J Magn Reson Imaging* 2014;40:596-602.
25. Damon BM, Froeling M, Buck AK, Oudeman J, Ding Z, Nederveen AJ, Bush EC, Strijkers GJ. Skeletal muscle diffusion tensor-MRI fiber tracking: rationale, data acquisition and analysis methods, applications and future directions. *NMR Biomed* 2016. [Epub ahead of print].
26. Chu CR, Williams AA, West RV, Qian Y, Fu FH, Do BH, Bruno S. Quantitative Magnetic Resonance Imaging UTE-T2* Mapping of Cartilage and Meniscus Healing After Anatomic Anterior Cruciate Ligament Reconstruction. *Am J Sports Med* 2014;42:1847-56.
27. Du J, Bydder M, Takahashi AM, Carl M, Chung CB, Bydder GM. Short T2 contrast with three-dimensional ultrashort echo time imaging. *Magn Reson Imaging* 2011;29:470-82.
28. Matzat SJ, Kogan F, Fong GW, Gold GE. Imaging strategies for assessing cartilage composition in osteoarthritis. *Curr Rheumatol Rep* 2014;16:462.
29. Roemer FW, Eckstein F, Hayashi D, Guermazi A. The role of imaging in osteoarthritis. *Best Pract Res Clin Rheumatol* 2014;28:31-60.
30. Wehrli FW, Song HK, Saha PK, Wright AC. Quantitative MRI for the assessment of bone structure and function. *NMR Biomed* 2006;19:731-64.
31. Hirsch FW, Sattler B, Sorge I, Kurch L, Viehweger A, Ritter L, Werner P, Jochimsen T, Barthel H, Bierbach U, Till H, Sabri O, Kluge R. PET/MR in children. Initial clinical experience in paediatric oncology using an integrated PET/MR scanner. *Pediatr Radiol* 2013;43:860-75.
32. Vandenberghe S, Marsden PK. PET-MRI: a review of challenges and solutions in the development of integrated multimodality imaging. *Phys Med Biol* 2015;60:R115-54.
33. Peng BH, Levin CS. Recent development in PET instrumentation. *Curr Pharm Biotechnol* 2010;11:555-71.
34. Zaidi H, Ojha N, Morich M, Griesmer J, Hu Z, Maniawski P, Ratib O, Izquierdo-Garcia D, Fayad ZA, Shao L. Design and performance evaluation of a whole-body Ingenuity TF PET-MRI system. *Phys Med Biol* 2011;56:3091-106.
35. Wu Y, Ng TS, Yang Y, Shah K, Farrell R, Cherry SR. A study of the timing properties of position-sensitive avalanche photodiodes. *Phys Med Biol* 2009;54:5155-72.
36. Roncali E, Cherry SR. Application of silicon photomultipliers to positron emission tomography. *Ann Biomed Eng* 2011;39:1358-77.
37. Wagenknecht G, Kaiser HJ, Mottaghy FM, Herzog H. MRI for attenuation correction in PET: methods and challenges. *MAGMA* 2013;26:99-113.
38. Hofmann M, Pichler B, Scholkopf B, Beyer T. Towards quantitative PET/MRI: a review of MR-based attenuation correction techniques. *Eur J Nucl Med Mol Imaging* 2009;36:S93-104.
39. Hofmann M, Steinke F, Scheel V, Charpiat G, Farquhar J, Aschoff P, Brady M, Schölkopf B, Pichler BJ. MRI-based attenuation correction for PET/MRI: a novel approach

- combining pattern recognition and atlas registration. *J Nucl Med* 2008;49:1875-83.
40. Paulus DH, Tellmann L, Quick HH. Towards improved hardware component attenuation correction in PET/MR hybrid imaging. *Phys Med Biol* 2013;58:8021-40.
 41. Jamar F, Buscombe J, Chiti A, Christian PE, Delbeke D, Donohoe KJ, Israel O, Martin-Comin J, Signore A. EANM/SNMMI guideline for 18F-FDG use in inflammation and infection. *J Nucl Med* 2013;54:647-58.
 42. Iagaru A, Mittra E, Minamimoto R, Jamali M, Levin C, Quon A, Gold G, Herfkens R, Vasanaawala S, Gambhir SS, Zaharchuk G. Simultaneous whole-body time-of-flight 18F-FDG PET/MRI: a pilot study comparing SUVmax with PET/CT and assessment of MR image quality. *Clin Nucl Med* 2015;40:1-8.
 43. Barbosa Fde G, von Schulthess G, Veit-Haibach P. Workflow in Simultaneous PET/MRI. *Semin Nucl Med* 2015;45:332-44.
 44. Boellaard R. Standards for PET image acquisition and quantitative data analysis. *J Nucl Med* 2009;50:11S-20S.
 45. Kinahan PE, Fletcher JW. Positron emission tomography-computed tomography standardized uptake values in clinical practice and assessing response to therapy. *Semin Ultrasound CT MR* 2010;31:496-505.
 46. Blake GM, Siddique M, Frost ML, Moore AE, Fogelman I. Quantitative PET Imaging Using (18)F Sodium Fluoride in the Assessment of Metabolic Bone Diseases and the Monitoring of Their Response to Therapy. *PET Clin* 2012;7:275-91.
 47. Gunn RN, Gunn SR, Turkheimer FE, Aston JA, Cunningham VJ. Positron emission tomography compartmental models: a basis pursuit strategy for kinetic modeling. *J Cereb Blood Flow Metab* 2002;22:1425-39.
 48. Bentourkia M, Zaidi H. Tracer Kinetic Modeling in PET. *PET Clin* 2007;2:267-77.
 49. Sari H, Erlandsson K, Thielemans K, Atkinson D, Arridge S, Ourselin S, Hutton B. Incorporation of MRI-AIF information for improved kinetic modelling of dynamic PET data. *EJNMMI Phys* 2014;1:A43.
 50. Oei EH, van Tiel J, Robinson WH, Gold GE. Quantitative radiological imaging techniques for articular cartilage composition: Towards early diagnosis and development of disease-modifying therapeutics for osteoarthritis. *Arthritis Care Res (Hoboken)* 2014;66:1129-41.
 51. Guermazi A, Burstein D, Conaghan P, Eckstein F, Hellio Le Graverand-Gastineau MP, Keen H, Roemer FW. Imaging in osteoarthritis. *Rheum Dis Clin North Am* 2008;34:645-87.
 52. Potter HG, Koff MF. MR Imaging Tools to Assess Cartilage and Joint Structures. *HSS J* 2012;8:29-32.
 53. Guermazi A, Roemer FW, Hayashi D, Crema MD, Niu J, Zhang Y, Marra MD, Katur A, Lynch JA, El-Khoury GY, Baker K, Hughes LB, Nevitt MC, Felson DT. Assessment of synovitis with contrast-enhanced MRI using a whole-joint semiquantitative scoring system in people with, or at high risk of, knee osteoarthritis: the MOST study. *Ann Rheum Dis* 2011;70:805-11.
 54. Hunter DJ, Guermazi A, Lo GH, Grainger AJ, Conaghan PG, Boudreau RM, Roemer FW. Evolution of semi-quantitative whole joint assessment of knee OA: MOAKS (MRI Osteoarthritis Knee Score). *Osteoarthritis Cartilage* 2011;19:990-1002.
 55. Felson DT, Lynch J, Guermazi A, Roemer FW, Niu J, McAlindon T, Nevitt MC. Comparison of BLOKS and WORMS scoring systems part II. Longitudinal assessment of knee MRIs for osteoarthritis and suggested approach based on their performance: data from the Osteoarthritis Initiative. *Osteoarthritis Cartilage* 2010;18:1402-7.
 56. Dardzinski BJ, Mosher TJ, Li S, Van Slyke MA, Smith MB. Spatial variation of T2 in human articular cartilage. *Radiology* 1997;205:546-50.
 57. Mosher TJ, Dardzinski BJ. Cartilage MRI T2 relaxation time mapping: overview and applications. *Semin Musculoskelet Radiol* 2004;8:355-68.
 58. Regatte RR, Akella SV, Borthakur A, Reddy R. Proton spin-lock ratio imaging for quantitation of glycosaminoglycans in articular cartilage. *J Magn Reson Imaging* 2003;17:114-21.
 59. Borthakur A, Mellon E, Niyogi S, Witschey W, Kneeland JB, Reddy R. Sodium and T1rho MRI for molecular and diagnostic imaging of articular cartilage. *NMR Biomed* 2006;19:781-821.
 60. Baldassarri M, Goodwin JS, Farley ML, Bierbaum BE, Goldring SR, Goldring MB, Burstein D, Gray ML. Relationship between cartilage stiffness and dGEMRIC index: correlation and prediction. *J Orthop Res* 2007;25:904-12.
 61. Trattig S, Marlovits S, Gebetsroither S, Szomolanyi P, Welsch GH, Salomonowitz E, Watanabe A, Deimling M, Mamisch TC. Three-dimensional delayed gadolinium-enhanced MRI of cartilage (dGEMRIC) for in vivo evaluation of reparative cartilage after matrix-associated autologous chondrocyte transplantation at 3.0T: Preliminary results. *J Magn Reson Imaging* 2007;26:974-82.
 62. Singh A, Haris M, Cai K, Kasey VB, Kogan F, Reddy D, Hariharan H, Reddy R. Chemical exchange saturation transfer magnetic resonance imaging of human knee

- cartilage at 3 T and 7 T. *Magn Reson Med* 2012;68:588-94.
63. Kogan F, Hargreaves BA, Gold GE. Volumetric multislice gagCEST imaging of articular cartilage: Optimization and comparison with T1rho. *Magn Reson Med* 2016. [Epub ahead of print].
 64. Burr DB, Gallant MA. Bone remodelling in osteoarthritis. *Nat Rev Rheumatol* 2012;8:665-73.
 65. Hayami T, Pickarski M, Wesolowski GA, McLane J, Bone A, Destefano J, Rodan GA, Duong LT. The role of subchondral bone remodeling in osteoarthritis: reduction of cartilage degeneration and prevention of osteophyte formation by alendronate in the rat anterior cruciate ligament transection model. *Arthritis Rheum* 2004;50:1193-206.
 66. Lee JW, Lee SM, Kim SJ, Choi JW, Baek KW. Clinical utility of fluoride-18 positron emission tomography/CT in temporomandibular disorder with osteoarthritis: comparisons with ^{99m}Tc-MDP bone scan. *Dentomaxillofac Radiol* 2013;42:29292350.
 67. Kobayashi N, Inaba Y, Tateishi U, Ike H, Kubota S, Inoue T, Saito T. Comparison of 18F-fluoride positron emission tomography and magnetic resonance imaging in evaluating early-stage osteoarthritis of the hip. *Nucl Med Commun* 2015;36:84-9.
 68. Draper CE, Fredericson M, Gold GE, Besier TF, Delp SL, Beaupre GS, Quon A. Patients with patellofemoral pain exhibit elevated bone metabolic activity at the patellofemoral joint. *J Orthop Res* 2012;30:209-13.
 69. Draper CE, Quon A, Fredericson M, Besier TF, Delp SL, Beaupre GS, Gold GE. Comparison of MRI and (1)(8) F-NaF PET/CT in patients with patellofemoral pain. *J Magn Reson Imaging* 2012;36:928-32.
 70. Hayashi D, Roemer FW, Katur A, Felson DT, Yang SO, Alomran F, Guermazi A. Imaging of synovitis in osteoarthritis: current status and outlook. *Semin Arthritis Rheum* 2011;41:116-30.
 71. Sellam J, Berenbaum F. The role of synovitis in pathophysiology and clinical symptoms of osteoarthritis. *Nat Rev Rheumatol* 2010;6:625-35.
 72. Nakamura H, Masuko K, Yudoh K, Kato T, Nishioka K, Sugihara T, Beppu M. Positron emission tomography with 18F-FDG in osteoarthritic knee. *Osteoarthritis Cartilage* 2007;15:673-81.
 73. Wandler E, Kramer EL, Sherman O, Babb J, Scarola J, Rafii M. Diffuse FDG shoulder uptake on PET is associated with clinical findings of osteoarthritis. *AJR Am J Roentgenol* 2005;185:797-803.
 74. Felson DT, Chaisson CE, Hill CL, Totterman SM, Gale ME, Skinner KM, Kazis L, Gale DR. The association of bone marrow lesions with pain in knee osteoarthritis. *Ann Intern Med* 2001;134:541-9.
 75. Kogan F, Fan AP, McWalter EJ, Quon A, Oei EH, Gold G. PET-MR imaging of metabolic bone activity in knee osteoarthritis. *Osteoarthritis and Cartilage* 2016;24:S318-9.
 76. Kogan F, Fan AP, McWalter EJ, Oei EHG, Quon A, Gold GE. PET/MRI of metabolic activity in osteoarthritis: A feasibility study. *J Magn Reson Imaging* 2016. [Epub ahead of print].
 77. Carey K, Saboury B, Basu S, Brothers A, Ogdie A, Werner T, Torigian DA, Alavi A. Evolving role of FDG PET imaging in assessing joint disorders: a systematic review. *Eur J Nucl Med Mol Imaging* 2011;38:1939-55.
 78. Beckers C, Ribbens C, André B, Marcelis S, Kaye O, Mathy L, Kaiser MJ, Hustinx R, Foidart J, Malaise MG. Assessment of disease activity in rheumatoid arthritis with (18)F-FDG PET. *J Nucl Med* 2004;45:956-64.
 79. Narvaez JA, Narvaez J, De Lama E, De Albert M. MR imaging of early rheumatoid arthritis. *Radiographics* 2010;30:143-63; discussion 63-5.
 80. Matsui T, Nakata N, Nagai S, Nakatani A, Takahashi M, Momose T, Ohtomo K, Koyasu S. Inflammatory cytokines and hypoxia contribute to 18F-FDG uptake by cells involved in pannus formation in rheumatoid arthritis. *J Nucl Med* 2009;50:920-6.
 81. Roivainen A, Parkkola R, Yli-Kerttula T, Lehtikainen P, Viljanen T, Möttönen T, Nuutila P, Minn H. Use of positron emission tomography with methyl-11C-choline and 2-18F-fluoro-2-deoxy-D-glucose in comparison with magnetic resonance imaging for the assessment of inflammatory proliferation of synovium. *Arthritis Rheum* 2003;48:3077-84.
 82. Zeman MN, Scott PJ. Current imaging strategies in rheumatoid arthritis. *Am J Nucl Med Mol Imaging* 2012;2:174-220.
 83. van der Laken CJ, Elzinga EH, Kropholler MA, Molthoff CF, van der Heijden JW, Maruyama K, Boellaard R, Dijkmans BA, Lammertsma AA, Voskuyl AE. Noninvasive imaging of macrophages in rheumatoid synovitis using 11C-(R)-PK11195 and positron emission tomography. *Arthritis Rheum* 2008;58:3350-5.
 84. Emery P. Evidence supporting the benefit of early intervention in rheumatoid arthritis. *J Rheumatol Suppl* 2002;66:3-8.
 85. Crowley AR, Dong J, McHaffie A, Clarke AW, Reeves Q, Williams M, Robinson E, Dalbeth N, McQueen FM. Measuring bone erosion and edema in rheumatoid arthritis:

- a comparison of manual segmentation and RAMRIS methods. *J Magn Reson Imaging* 2011;33:364-71.
86. Hodgson RJ, Connolly S, Barnes T, Eyes B, Campbell RS, Moots R. Pharmacokinetic modeling of dynamic contrast-enhanced MRI of the hand and wrist in rheumatoid arthritis and the response to anti-tumor necrosis factor-alpha therapy. *Magn Reson Med* 2007;58:482-9.
 87. Elzinga EH, van der Laken CJ, Comans EF, Lammertsma AA, Dijkmans BA, Voskuyl AE. 2-Deoxy-2-[F-18]fluoro-D-glucose joint uptake on positron emission tomography images: rheumatoid arthritis versus osteoarthritis. *Mol Imaging Biol* 2007;9:357-60.
 88. McQueen FM, Ostergaard M. Established rheumatoid arthritis - new imaging modalities. *Best Pract Res Clin Rheumatol* 2007;21:841-56.
 89. Miese F, Scherer A, Ostendorf B, Heinzl A, Lanzman RS, Kröpil P, Blondin D, Hautzel H, Wittsack HJ, Schneider M, Antoch G, Herzog H, Shah NJ. Hybrid 18F-FDG PET-MRI of the hand in rheumatoid arthritis: initial results. *Clin Rheumatol* 2011;30:1247-50.
 90. Cook GJ, Fogelman I. The role of positron emission tomography in skeletal disease. *Semin Nucl Med* 2001;31:50-61.
 91. Li ZC, Jiang SD, Yan J, Jiang LS, Dai LY. Small-animal PET/CT assessment of bone microdamage in ovariectomized rats. *J Nucl Med* 2011;52:769-75.
 92. Kurata S, Shizukuishi K, Tateishi U, Yoneyama T, Hino A, Ishibashi M, Inoue T. Age-related changes in pre- and postmenopausal women investigated with 18F-fluoride PET--a preliminary study. *Skeletal Radiol* 2012;41:947-53.
 93. Kato K, Aoki J, Endo K. Utility of FDG-PET in differential diagnosis of benign and malignant fractures in acute to subacute phase. *Ann Nucl Med* 2003;17:41-6.
 94. Schmitz A, Risse JH, Textor J, Zander D, Biersack HJ, Schmitt O, Palmedo H. FDG-PET findings of vertebral compression fractures in osteoporosis: preliminary results. *Osteoporos Int* 2002;13:755-61.
 95. Link TM. Osteoporosis imaging: state of the art and advanced imaging. *Radiology* 2012;263:3-17.
 96. Adams JE. Advances in bone imaging for osteoporosis. *Nat Rev Endocrinol* 2013;9:28-42.
 97. Manhard MK, Horch RA, Gochberg DF, Nyman JS, Does MD. In Vivo Quantitative MR Imaging of Bound and Pore Water in Cortical Bone. *Radiology* 2015;277:221-9.
 98. Rad HS, Lam SC, Magland JF, Ong H, Li C, Song HK, Love J, Wehrli FW. Quantifying cortical bone water in vivo by three-dimensional ultra-short echo-time MRI. *NMR Biomed* 2011;24:855-64.
 99. Li C, Seifert AC, Rad HS, Bhagat YA, Rajapakse CS, Sun W, Benny Lam SC, Wehrli FW. Cortical Bone Water Concentration: Dependence of MR Imaging Measures on Age and Pore Volume Fraction. *Radiology* 2016;280:653.
 100. Ito M. Recent progress in bone imaging for osteoporosis research. *J Bone Miner Metab* 2011;29:131-40.
 101. Pistoia W, van Rietbergen B, Lochmuller EM, Lill CA, Eckstein F, Ruegsegger P. Image-based micro-finite-element modeling for improved distal radius strength diagnosis: moving from bench to bedside. *J Clin Densitom* 2004;7:153-60.
 102. Koivumäki JE, Thevenot J, Pulkkinen P, Kuhn V, Link TM, Eckstein F, Jämsä T. Cortical bone finite element models in the estimation of experimentally measured failure loads in the proximal femur. *Bone* 2012;51:737-40.
 103. Zhang N, Magland JF, Rajapakse CS, Lam SB, Wehrli FW. Assessment of trabecular bone yield and post-yield behavior from high-resolution MRI-based nonlinear finite element analysis at the distal radius of premenopausal and postmenopausal women susceptible to osteoporosis. *Acad Radiol* 2013;20:1584-91.
 104. Chang G, Rajapakse CS, Diamond M, Honig S, Recht MP, Weiss DS, Regatte RR. Micro-finite element analysis applied to high-resolution MRI reveals improved bone mechanical competence in the distal femur of female pre-professional dancers. *Osteoporos Int* 2013;24:1407-17.
 105. Jensen MC, Brant-Zawadzki MN, Obuchowski N, Modic MT, Malkasian D, Ross JS. Magnetic resonance imaging of the lumbar spine in people without back pain. *N Engl J Med* 1994;331:69-73.
 106. Sher JS, Uribe JW, Posada A, Murphy BJ, Zlatkin MB. Abnormal findings on magnetic resonance images of asymptomatic shoulders. *J Bone Joint Surg Am* 1995;77:10-5.
 107. Behera D, Jacobs KE, Behera S, Rosenberg J, Biswal S. (18)F-FDG PET/MRI can be used to identify injured peripheral nerves in a model of neuropathic pain. *J Nucl Med* 2011;52:1308-12.
 108. Cheng G, Chamroonrat W, Bing Z, Huang S, Zhuang H. Elevated FDG activity in the spinal cord and the sciatic nerves due to neuropathy. *Clin Nucl Med* 2009;34:950-1.
 109. Imamoto N, Momosaki S, Fujita M, Omachi S, Yamato H, Kimura M, Kanegawa N, Shinohara S, Abe K. [11C] PK11195 PET imaging of spinal glial activation after nerve injury in rats. *Neuroimage* 2013;79:121-8.
 110. James ML, Shen B, Nielsen CH, Behera D, Buckmaster CL, Mesangeau C, Zavaleta C, Vuppala PK, Jamalapuram S, Avery BA, Lyons DM, McCurdy CR, Biswal S, Gambhir

- SS, Chin FT. Evaluation of sigma-1 receptor radioligand 18F-FTC-146 in rats and squirrel monkeys using PET. *J Nucl Med* 2014;55:147-53.
111. Ghanouni P, Behera D, Xie J, Chen X, Moseley M, Biswal S. In vivo USPIO magnetic resonance imaging shows that minocycline mitigates macrophage recruitment to a peripheral nerve injury. *Mol Pain* 2012;8:49.
112. Ohana M, Moser T, Moussaoui A, Kremer S, Carlier RY, Liverneux P, Dietemann JL. Current and future imaging of the peripheral nervous system. *Diagn Interv Imaging* 2014;95:17-26.
113. Stoll G, Bendszus M, Perez J, Pham M. Magnetic resonance imaging of the peripheral nervous system. *J Neurol* 2009;256:1043-51.
114. Biswal S, Behera D, Yoon DH, Holley D, Ith MA, Carroll I, Smuck M, Hargreaves B. [18F]FDG PET/MRI of patients with chronic pain alters management: early experience. *EJNMMI Phys* 2015;2:A84.
115. Parthipun A, Moser J, Mok W, Paramithas A, Hamilton P, Sott AH. 99mTc-HDP SPECT-CT Aids Localization of Joint Injections in Degenerative Joint Disease of the Foot and Ankle. *Foot Ankle Int* 2015;36:928-35.
116. Schipilow JD, Macdonald HM, Liphardt AM, Kan M, Boyd SK. Bone micro-architecture, estimated bone strength, and the muscle-bone interaction in elite athletes: an HR-pQCT study. *Bone* 2013;56:281-9.
117. Paluch L, Nawrocka-Laskus E, Wiczorek J, Mruk B, Frel M, Walecki J. Use of Ultrasound Elastography in the Assessment of the Musculoskeletal System. *Pol J Radiol* 2016;81:240-6.
118. Zaheer A, Lenkinski RE, Mahmood A, Jones AG, Cantley LC, Frangioni JV. In vivo near-infrared fluorescence imaging of osteoblastic activity. *Nat Biotechnol* 2001;19:1148-54.

Cite this article as: Kogan F, Fan AP, Gold GE. Potential of PET-MRI for imaging of non-oncologic musculoskeletal disease. *Quant Imaging Med Surg* 2016;6(6):756-771. doi: 10.21037/qims.2016.12.16